CEAS-GNC-2022-037

CEAS EuroGNC 2022
"Conference on Guidance, Navigation and Control"
3-5 May 2022 @ Technische Universität Berlin, Germany

The Vortex Position Estimator used for the Airbus fello'fly Transatlantic Crossing

Jordan Adams Airbus, Toulouse, France. Jordan.Adams@airbus.com

Clément Frot Airbus, Toulouse, France. Clement.Frot@airbus.com

Guillaume Ta Airbus, Toulouse, France. Guillaume.Ta@Airbus.com

ABSTRACT

In November 2021 the Airbus fello'fly project completed two transatlantic formation flights demonstrating a reduction of fuel consumption of 5% trip fuel for the follower. The follower achieved this by maintaining an optimum lateral position relative to the wake vortices generated by the leader. The flights were achieved automatically via the existing auto flight system, modified such that commands to the autopilot outer loops could be provided by additional real-time computers. A dedicated data-link was also installed for aircraft to aircraft communication of parameters. The computation of the relative position feedbacks for the control loops were based on a geometric model of the wake vortex propagation. Due to assumptions in the propagation model, and the precision of the source data, this initial position estimate could not be sufficiently accurate for maintaining the fuel saving position. To achieve the required accuracy, an additional indirect measurement of the vortex position was obtained by combining a model of the aircraft trim with a parametric model of the rolling moment induced by the vortices on the follower. A four state model of the system was constructed, including two states for the position bias obtained from the geometric wake position model, one state for the shape of the vortex effect map, and one state for the aircraft lateral trim bias. Estimation of the position was achieved with a bootstrap particle filter, wherein the importance sampling distribution was based on the prior distribution. A resampling step was performed whenever a computed indicator of the degeneracy of the particle weights decreased below a threshold. The resampling was performed using a multinomial systematic resampling algorithm.

Keywords: Formation flight; Bootstrap particle filter; fello'fly; Wake surfing

Nomenclature

ADS	=	Air Data System
GNSS	=	Global Navigation Satellite System
HIL	=	Hardware In the Loop
IMU,	=	Inertial Measurement Unit
$\dot{P}$	=	Angular acceleration in the roll axis
PVE	=	Parametric Vortex Effect model
WER	=	Wake Energy Retrieval
ΔC_l	=	Incremental aerodynamic rolling moment coefficent
Λ_z	=	PVE map asymmetry parameter

1 Introduction

The Airbus fello'fly project completed a pair of transatlantic demonstration flights in November 2021. The flights were performed by an A350-900 and an A350-1000 from Airbus' fleet of flight test aircraft, fulfilling the roles of leader and follower respectively. The aim was to demonstrate the technical and operational feasibility of formation flights performing wake energy retrieval (WER) using large commercial airliners. The flights were successful, achieving a 5% reduction in the trip fuel consumption while operating in non-segregated airspace. While such benefits have been demonstrated in the past [1, 2, 3, 4], the transatlantic demonstration flights were a first for modern wide body airliners in non-segregated airspace representing realistic commercial passenger operations.

WER is achieved by positioning a following aircraft nearby the wake vortex pair generated by a leading aircraft. Considering the relative positions as defined in Figure 1, the optimal position is at the same altitude as the wake ($\Delta z = 0$), with the follower outboard of the wake vortices. In this position, the wing of the follower is exposed to the rising airflow of the wake. This has several effects, the most important being the upward rotation of the local relative air velocity vector ($\vec{U}_x \rightarrow \vec{U}_i$) seen along the wing. Simply put, this rotates the local aerodynamic force vector such that the net aerodynamic drag is reduced.

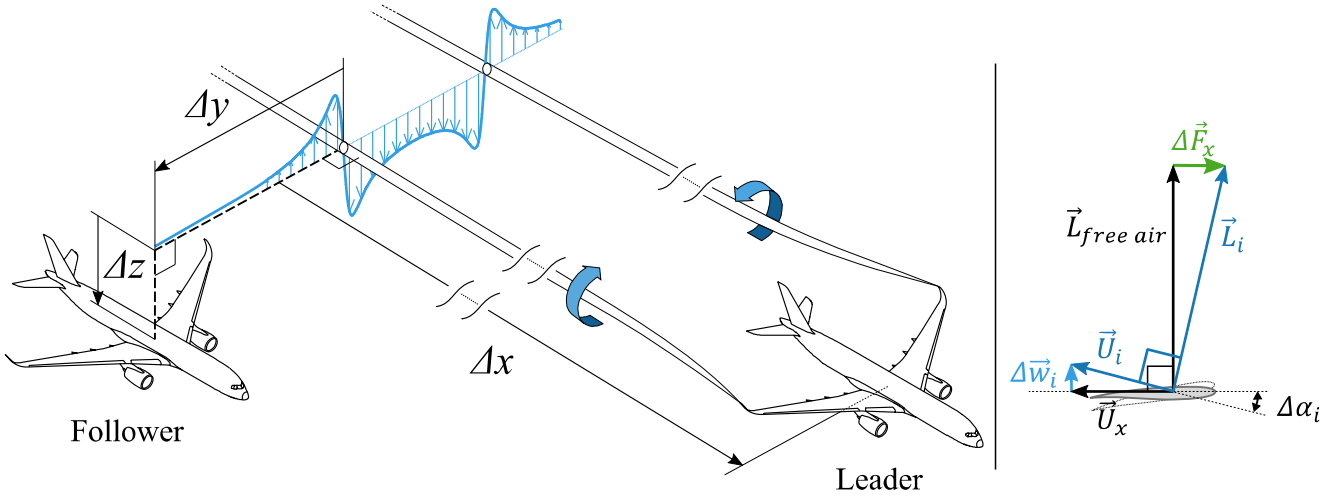

Fig. 1 Definition of formation relative geometry parameters (left). The flow field induced by the wake vortex pair at $\Delta z = 0$ is shown in blue. Right, a vector diagram shows the rotation of the local section lift by the wake upwash ($\Delta\vec{w}_i$), resulting in a beneficial force component ($\Delta\vec{F}_x$) in the direction of flight.

The aerodynamic effects are strongly sensitive to the relative position of the follower with respect to the wake, with the induced velocity field following an inverse square relationship as a function of distance from the vortex cores. This results in asymmetry of the induced aerodynamic loads which must be trimmed via lateral control inputs. At very close distances to the wake, the non-linearity of the induced loads combined with the variability of the vortex position (and other vibrations induced by the vortex) begins to impact the high levels of comfort expected in the cabin. This leads to a trade-off between fuel gains and comfort levels which is best managed through a variable target, tunable by the crew. The technical challenge was to automatically find and maintain this target position relative to the wake vortices such that the fuel saving benefits can be realized. Furthermore, the fello'fly demonstrator aimed to do this without the use of additional sensors. Various algorithms have been proposed to achieve this, either by applying optimisation algorithms [5, 6] or through the use of modern estimation methods [7]. This paper focuses on the design of the bootstrap particle filter used to address this challenge.

2 Relative Position Models of the Wake Vortices

The first step in the wake relative position computation is a geometric model of the wake propagation calculated on the follower aircraft. Here, the leader's latitude and longitude, wind speed and wind direction received via a datalink are recorded in a stack. Wake propagation is modeled by linear advection assuming a frozen wind and turbulence field. This stack is transformed into a 3D representation of the vortex core positions by assuming linear advection of the initial rolled-up vortex cores in a frozen wind and turbulence field. The initial vortex geometry is identified for the specific leader aircraft with sufficient precision from classical linear theory [8] by considering the wingspan and appropriate span loading. The relative position of the follower is then the minimum relative distance vector between the follower position and the stack of points representing the wake. This vector is decomposed into Δy_G and Δz_G in an axis system defined by the cross product of the gravity vector with the rotation axis of the closest vortex (projected onto the horizontal plane).

The input position and wind data are the optimal result of hybridization algorithms embedded in the onboard systems of each aircraft (IMU, ADS, GNSS). While precise and reliable for normal operational and navigation requirements, the input data and propagation model can only provide an initial estimate of the relative wake vortex positions. This is subject to errors, noise and biases which evolve significantly over time. The key to maintaining position in close proximity is to estimate and track these biases, $b_{\Delta y}$ and $b_{\Delta z}$, indicated in Figure 2:

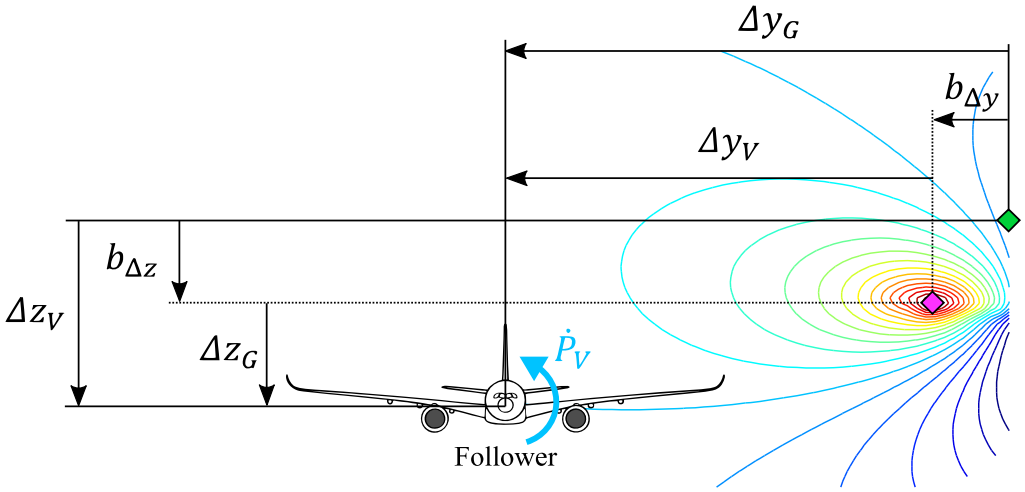

Fig. 2 Position biases $b_{\Delta y}$ and $b_{\Delta z}$ between the actual vortex position (magenta diamond) and the geometric wake propagation model (green diamond). The contours indicate the map of the rolling acceleration $\dot{P}_V(\Delta y_V, \Delta z_V)$ induced by the vortex if the follower was not trimmed.

To achieve the accuracy needed for relative distance control, an additional indirect measurement of the vortex position is required. To this end, an analytical model of the expected vortex induced rolling moment was developed called the Parametric Vortex Effect (PVE) model. This could provide a value for the expected induced rolling coefficient $\Delta C_{l_{PVE}}$ as a function of Δy_V and Δz_V. The PVE depends on a range of parameters which characterize the geometry and strength of the vortex, as well as simplified geometric and performance characteristics of the follower's lifting surfaces. All of the free parameters of the PVE could be determined with high confidence with the exception of one, Λ_z, which represents the amount of asymmetry of the $\Delta C_{l_{PVE}}$ map above and below the line $\Delta z_V = 0$. This would mainly be influenced by the specific wing loading of the follower, wing bending and trim for a given flight condition.

By converting $\Delta C_{l_{PVE}}$ into an expected lateral roll acceleration $\dot{P}_{PVE}$, a comparison could be made with the actual roll disturbance as measured in flight. This is constructed as shown in in Equation 1:

$$\dot{P}_V = \dot{P}_S - \dot{P}_{FAM} \tag{1}$$

Here, $\dot{P}_V$ is the roll acceleration attributed to the wake vortex and $\dot{P}_S$ is that measured by the aircraft systems (IMU). To account for the deflection of the control surfaces, aerodynamic and inertial models of the follower aircraft were fed with the necessary aircraft state parameters in real time. This gives the expected roll angular acceleration in "free-air" from the models, $\dot{P}_{FAM}$. Due to small uncertainties in the aircraft's loading, engine trim and sensor inaccuracies, a small residual bias, $b_{\dot{P}}$, would be observed in free-air far from the wake vortices.

It is important to note that measuring a specific value of $\dot{P}_V$ determines which contour of the scalar map the follower is observing, and not a specific Δy_V or Δz_V location. It is therefore necessary to accumulate $\dot{P}_V$ measurements at range of relative positions in order to isolate a specific position. Given the uncertainties and biases present in the models, an appropriate estimation strategy is needed.

3 Bootstrap Particle Filter Design for a Wake Vortex Position Estimator

A simplified block diagram of the flight test architecture is shown below in Figure 3.

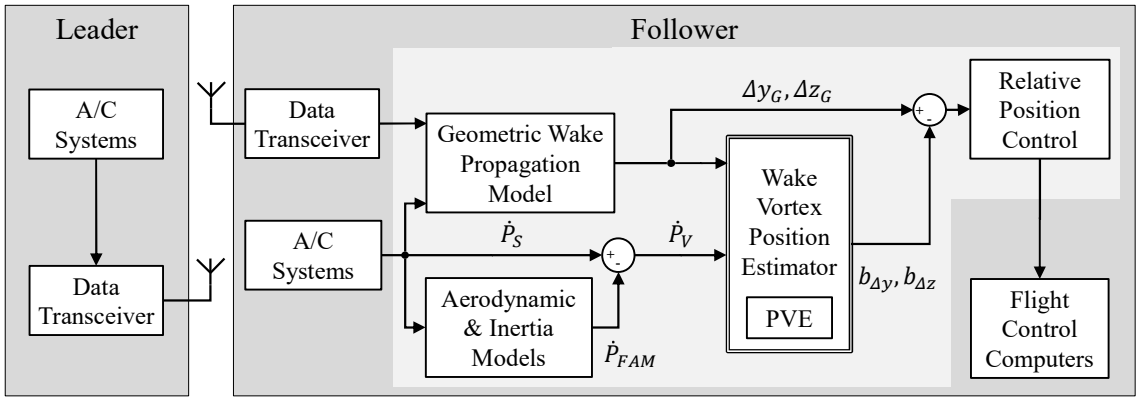

Fig. 3 Simplified block diagram indicating the main data flows in and out of the bootstrap particle filter.

In selecting the type of estimator to apply, four key features of the problem were considered:

1) The vortex effects are highly non-linear with respect to the uncertain relative position of the wake.
2) The uncertainty in the initial relative position is associated with a weakly observable measurement of the vortex-induced rolling effect.
3) Time-varying biases are present in the system, at time-scales similar to the system dynamics.
4) The map of the induced rolling effect is a 2D scalar field dependent on both the vertical and lateral separations, with $\frac{\partial \Delta C_l}{\partial \Delta z} \approx 0$ near $\Delta z_G = 0$ (i.e. at the same level as the vortex shown in Figure 2).

These features together make the problem ill-suited to Kalman filters and their extensions. Instead, a bootstrap particle filter was selected. A bootstrap particle filter is a type of Monte Carlo state estimation method [9]. The space of uncertainty of the system states is sampled with a large number of particles, N, in which the system dynamics are simulated in discrete steps. Its defining characteristic is that the importance sampling distribution is based on the transition prior distribution. That is to say, the particle weights are updated at each iteration for each particle based on its previous weight and its likelihood given the most recent measurement. Figure 4 shows the flow diagram of the bootstrap particle filter.

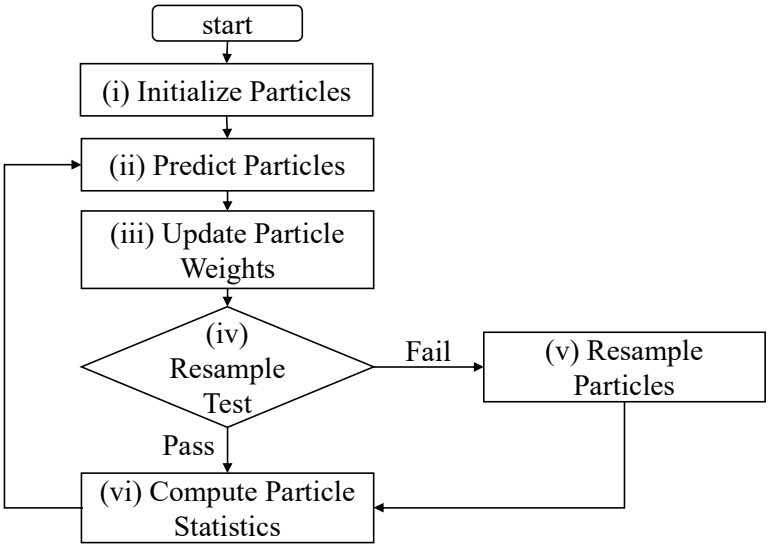

Fig. 4 Simplified block diagram indicating the main data flows in and out of the bootstrap particle filter.

During (i), at $k = 0$, N particles are drawn uniformly across the range of uncertainty known for each of the states, and each particle is weighted equally with $w_i(0) = 1/N$. From the models defined in the previous chapter, the state vector x and measurement vector z of the hidden Markov model were defined:

$$x = \begin{Bmatrix} b_{\Delta y} \\ b_{\Delta z} \\ b_{\dot{P}} \\ \Lambda_z \end{Bmatrix}, \quad z = \begin{Bmatrix} \Delta y_G \\ \Delta z_G \\ \dot{P}_V \end{Bmatrix} \tag{2}$$

At (ii) the particles must be propagated according to their respective state equations. This is achieved by simulating a transition for each particle with the transition prior probability distribution function $p(x_k|x_{k-1})$. The transition is simulated in real time by assuming that $p(x_k|x_{k-1})$ is distributed according to a multivariate normal distribution with independence between the components.

The particle weights are updated at step (iii). With the bootstrap particle filter, it is assumed that the set of N particles at step $k-1$ have a weight $w_{1:N}(k-1)$ which are sampled from $p(x_{0:k-1}|z_{0:k-1})$. Then, the weight of each particle is updated as follows:

$$w_i(k) = w_i(k-1).\overbrace{p(z_k|x_k)}^{likelihood} \tag{4}$$

The weights are subsequently normalized such that:

$$\sum_i w_i\,(k) = 1$$

According to Equation (A1) in the Appendix, the new set of particles and weight vector is sampled according to the probability distribution function $p(x_{0:k}|z_{0:k})$.

At step (iv) a resampling test is performed based on a computed indicator of the degeneracy of the particle weights. If this falls below a threshold, resampling is performed in step (v). The resampling is performed using a multinomial systematic resampling algorithm [10]. Finally in step (vi) the particle statistics are computed based on their weights. This reveals the probability distribution for each of the estimated states, and allows the means and confidence intervals to be determined. These are output from the particle filter after each calculation cycle, and used to correct Δy_G and Δz_G.

4 Estimator Convergence during Vortex Approach

The approach to the vortex is performed in two steps. The first step occurs far from the vortex effects with the follower aircraft stabilized laterally on a parallel trajectory to the leader. Here, there should be no vortex effect so $\dot{P}_V \cong 0$ and so $b_{\dot{P}} = \dot{P}_S - \dot{P}_{FAM}$. From this stabilized position, the bootstrap particle filter can be initialized and the rolling acceleration bias is quickly identified.

During the approach to the vortex it is necessary to perform a combination of vertical and lateral maneuvers in order to scan the zone of uncertainty in $b_{\Delta y}$ and $b_{\Delta z}$. This allows the probability distribution to converge on both the vertical and lateral vortex position as measurements of $\dot{P}_V$ are accumulated. In Figure 4 an illustrative, simulated approach is shown where the convergence of the estimator can be observed. The maximum and minimum positions are defined by the confidence windows computed from the probability distribution as sampled by the N particles.

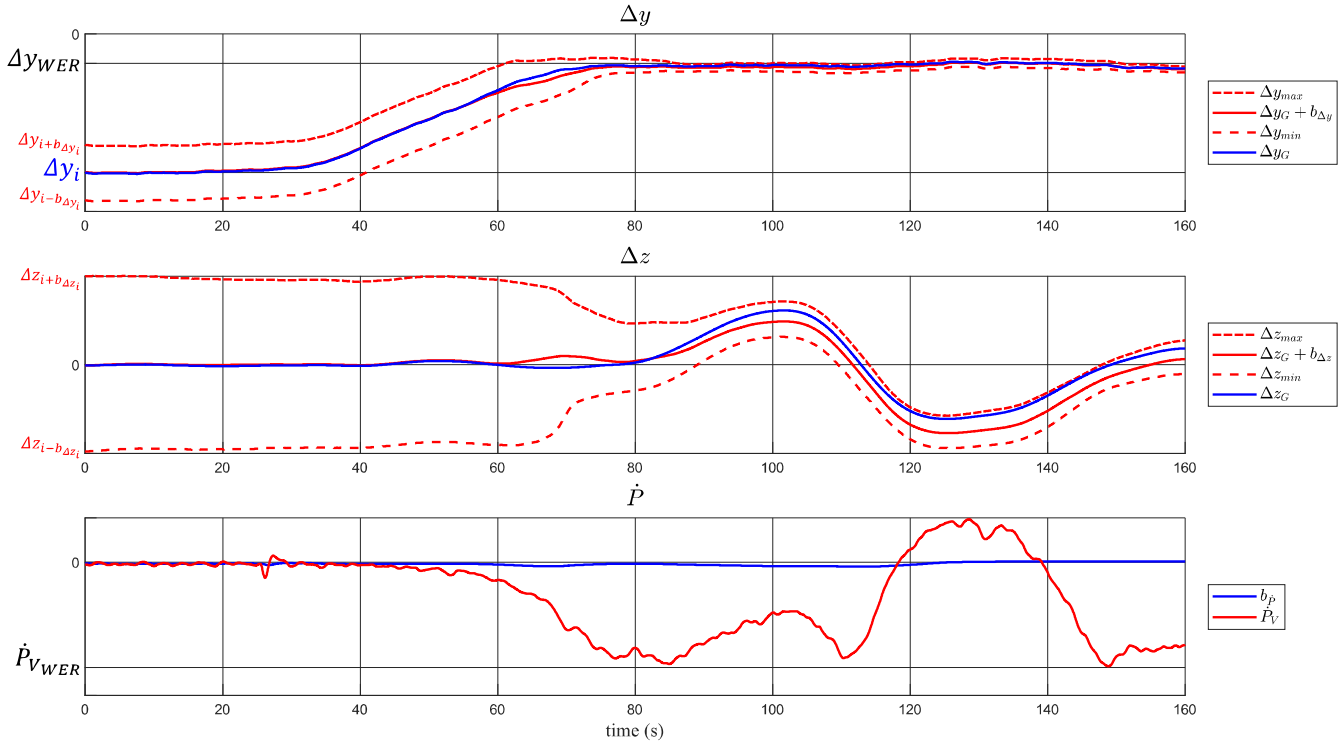

Fig. 4 An example simulation result showing convergence of the particle filter with light turbulence injection. Axis scales and dynamics are for illustration only.

At $t = 0$, the initial uncertainties $\pm\, b_{\Delta y_i}$ and $\pm\, b_{\Delta z_i}$ are initialised around $\Delta y_i = \Delta y_G$ and $\Delta z_i = \Delta z_G$. Within this zone of confidence, the N particles are initialised. A very small bias on the lateral roll acceleration has been quickly identified at the initial position far from the vortex influence.

After $t = 20\ s$, the flight control laws have targeted a desired lateral WER position, Δy_{WER}, and the initial lateral approach begins. At $t = 60\ s$ the induced roll acceleration measurement $\dot{P}_V$ becomes significant, and the region of uncertainty begins to converge, with the biases $b_{\Delta y}$ and $b_{\Delta z}$ reducing around the estimated position $(\Delta y, \Delta z)$. Just prior to $t = 80\ s$ a vertical movement is commanded and the aircraft begins to move vertically within the region of the vortex influence. Subsequently, the uncertainty in the vertical position of the vortex is observed to reduce. The expected vortex induced roll acceleration influence in the WER position ($\dot{P}_{V_{WER}}$) is indicated to illustrate that when the WER position is reached in Delta_y and Delta_z, the maximum expected lateral trim offset is achieved (in the absolute sense).

5 Validation and Tuning

For flight monitoring and validation, additional sensors were installed on the follower aircraft. This included wing tip booms for recording disturbances in the local freestream velocity, and a LiDAR capable of determining the positon of the wake vortex cores. Initial flight tests provided the dataset necessary to validate the aerodynamic models used to characterize the wake vortices and their influence on the follower. This same data could also be used within a simulation environment (HIL) in which the wake vortex position estimation algorithms could be evaluated. This enabled rapid development, tuning and benchmarking of the bootstrap particle filter against alternative estimator designs (EKF, UKF). These development tools ensured that the integration of the position estimation algorithms were matured during each phase of the flight testing plan. Furthermore, real-time health monitoring metrics and displays were developed and tested using these tools.

Prior to the final flight test phase, an additional toolset was developed which was capable of performing simulated flights behind leaders based on data in a library of long flights recorded on Airbus' flight test fleet. This represented over 115 hours of flight data in typical cruise operating conditions. These flights provided valuable performance characterization for the estimator in a range of realistic flight conditions. Exhaustive use of these validation tools ensured that no failures of the wake position estimator were observed during the transatlantic flights.

6 Conclusions

The bootstrap particle filter designed for the Airbus fello'fly project has shown excellent performance in enabling WER in real-world flight conditions. Further refinements and optimization of the algorithms continue to be investigated as the technology matures towards industrialization.

Appendix

The derivation of the update equation presented here follows that presented in [9]. The subscript notation $x_{0:k}$, indicates the values of the states and measures between step 0 and step k. Bayes theorem gives:

$$p(x_{0:k}|z_{0:k}) = \frac{p(z_{0:k}|x_{0:k}).p(x_{0:k})}{p(z_{0:k})}$$

where:

$$\begin{cases} p(x_{0:k}) = p(x_{0:k-1}).p(x_k|x_{0:k-1}) \\ p(z_{0:k}|x_{0:k}) = p(z_{0:k-1}|x_{0:k}).p(z_k|z_{0:k-1}; x_{0:k}) \\ p(z_{0:k}) = p(z_{0:k-1}).p(z_k|z_{0:k-1}) \end{cases}$$

Under a first order Markov chain assumption:

$$\begin{cases} p(x_k|x_{0:k-1}) = p(x_k|x_{k-1}) \\ p(z_k|z_{0:k-1}; x_{0:k}) = p(z_k|x_k) \\ p(z_{0:k-1}|x_{0:k}) = p(z_{0:k-1}|x_{0:k-1}) \end{cases}$$

It is deduced that:

$$\begin{cases} p(x_{0:k}) = p(x_{0:k-1}).p(x_k|x_{k-1}) \\ p(z_{0:k}|x_{0:k}) = p(z_{0:k-1}|x_{0:k-1}).p(z_k|x_k) \end{cases}$$

$$p(x_{0:k}|z_{0:k}) = \frac{p(z_{0:k-1}|x_{0:k-1}).p(x_{0:k-1}).p(x_k|x_{k-1}).p(z_k|x_k)}{p(z_{0:k-1}).p(z_k|z_{0:k-1})}$$

$$p(x_{0:k}|z_{0:k}) = \frac{p(x_{0:k-1}|z_{0:k-1}).p(x_k|x_{k-1}).p(z_k|x_k)}{p(z_k|z_{0:k-1})}$$

$$p(x_{0:k}|z_{0:k}) = p(x_{0:k-1}|z_{0:k-1}).\frac{\overbrace{p(x_k|x_{k-1})}^{transition\ prior} .\overbrace{p(z_k|x_k)}^{likelihood}}{\underbrace{p(z_k|z_{0:k-1})}_{normalization\ constant}} \quad \text{(A1)}$$

It can be observed that the normalization constant $p(z_k|z_{0:k-1})$ is not important in the present application because it is the same factor for all particles. Particle weights were simply normalized at the end of the weight update process.

References

[1] M. Vachon, R. Ray, K. Walsh, and K. Ennix. F/A-18 Aircraft Performance Benefits Measured during the Autonomous Formation Flight Project. TM-2003-210734, NASA, 2002.

[2] J. Pahle, D. Berger, M.W. Venti, J.J Faber, C. Duggan, and K. Cardinal. A preliminary flight investigation of formation flight for drag reduction on the C-17 aircraft. *AIAA Atmospheric Flight Mechanics Conference*. NASA Dryden Flight Research Center, August 2012.

[3] C. E. Hanson, J. Pahle, J. R. Reynolds, S. Andrade and B. Nelson. Experimental Measurements of Fuel Savings During Aircraft Wake Surfing. *AIAA Atmospheric Flight Mechanics Conference*, June 2018.

[4] G. Norris. Boeing/FedEx 777 Test Confirms Wake Fuel-Burn Benefit. *Aviation Week Network*. 13 December 2019.

[5] D. F. Chichka, J. L. Speyer, C. Fanti, and C. G. Park. Peak-Seeking Control for Drag Reduction in Formation Flight. *Journal of Guidance, Control, and Dynamics*, Vol. 29, No. 5, 2006, pp. 1221–1230.

[6] P. Binetti, K. B. Ariyur, M. Krstic, and F. Bernelli. Formation Flight Optimization Using Extremum Seeking Feedback. *Journal of Guidance, Control, and Dynamics*, Vol. 26, No. 1, 2003, pp. 132–142.

[7] I. Ransquin, D. G. Caprace, M. Duponcheel, and P. Chatelain. Wake Vortex Detection and Tracking for Aircraft Formation Flight. *Journal of Guidance, Control, and Dynamics*, Vol 44, No. 12, 2021, pp. 2225-2243.

[8] A. Betz. Behavior of vortex systems. Technical Report NACA-TM-713. June 1933.

[9] Nicolas Chopin , and Omiros Papaspiliopoulos. *An Introduction to Sequential Monte Carlo*. Springer, 2020.

[10] Douc, Randal, and Olivier Cappé. Comparison of resampling schemes for particle filtering. *Proceedings of the 4th International Symposium on Image and Signal Processing and Analysis,* 2005, pp. 64-69.